Flexural deformation in post-orogenic settings

Started with model for active-rifting (Kusznir et al., 1991)

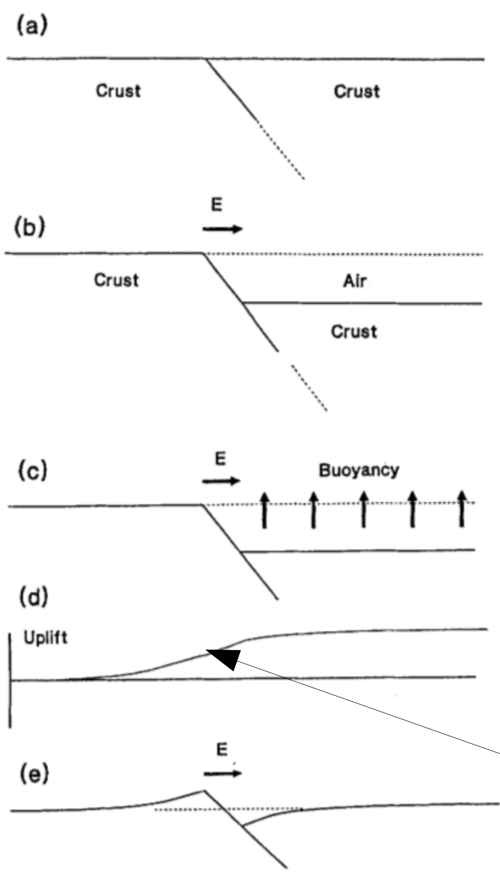

Fig. A2. Diagram summarizing the flexural isostatic interaction of foot-and hangingwall blocks during extension on a planar fault, neglecting the density contrast across the Moho between crust and mantle. See text for further explanation.

This buoyancy force gradient generates the rebound on the footwall,

which makes “empty” space

that must be filled with ductile crust.

addtl. flux result of pure shear thinning

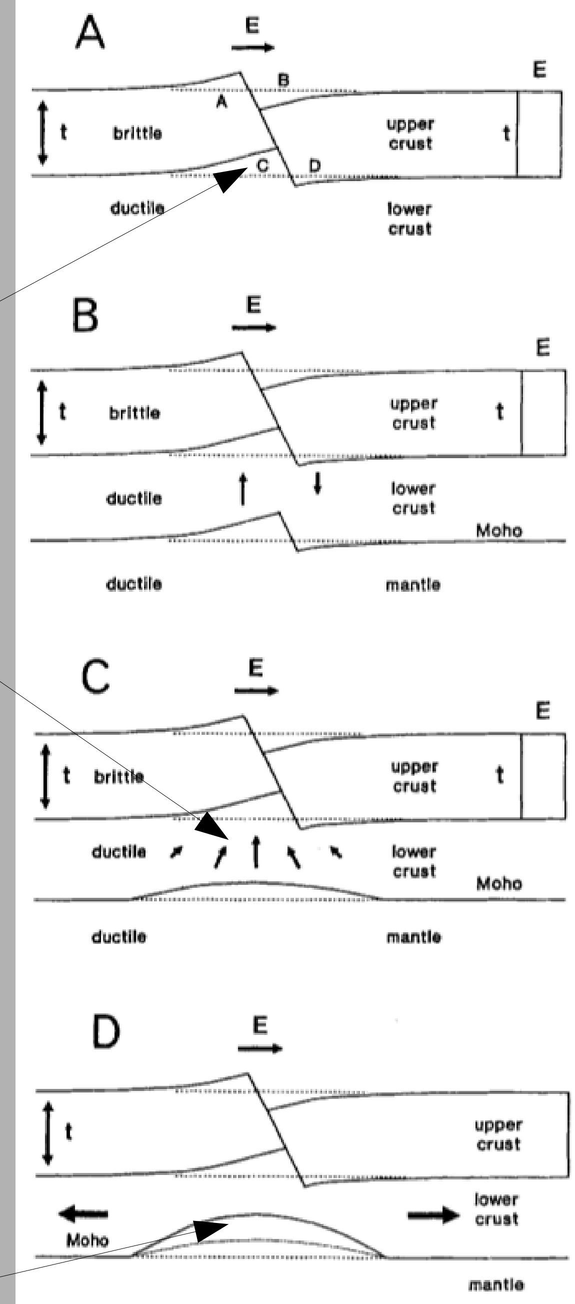

Fig. A3. Diagram summarizing mass conservation requirements following brittle, upper-crustal extension and the associated ductile flow in the lower crust and mantle and consequent perturbation of the Moho. See text for further explanation.

Basic equations governing the flexural deformation

buoyancy force

crustal surface

$$l_b(x) = -u(x)\ \rho_c\ g$$

Fourier transform

isostatic response function

$$R(k) = 1/((\rho_c - \rho_a)\ g + Dk^4)$$

flexural rigidity

k = wavenumber

$$W_b(k) = R(k)\ L_b(x)$$

flexural isostatic uplift

Fourier transform

$w_b(x)$ = flexural uplift response

Why did we read this?

- I think the paper sets up nicely, the governing equations for ALL flexural deformation studies.
- The force for deformation differs
  - In this case, it is a buoyancy force driven by extension
  - in other models it will be due to applied vertical loads

Kusznir et al., 1991. Flexural cantilever model for continental lithosphere extension, Appendix A.

Pazzaglia and Gardner, 1994

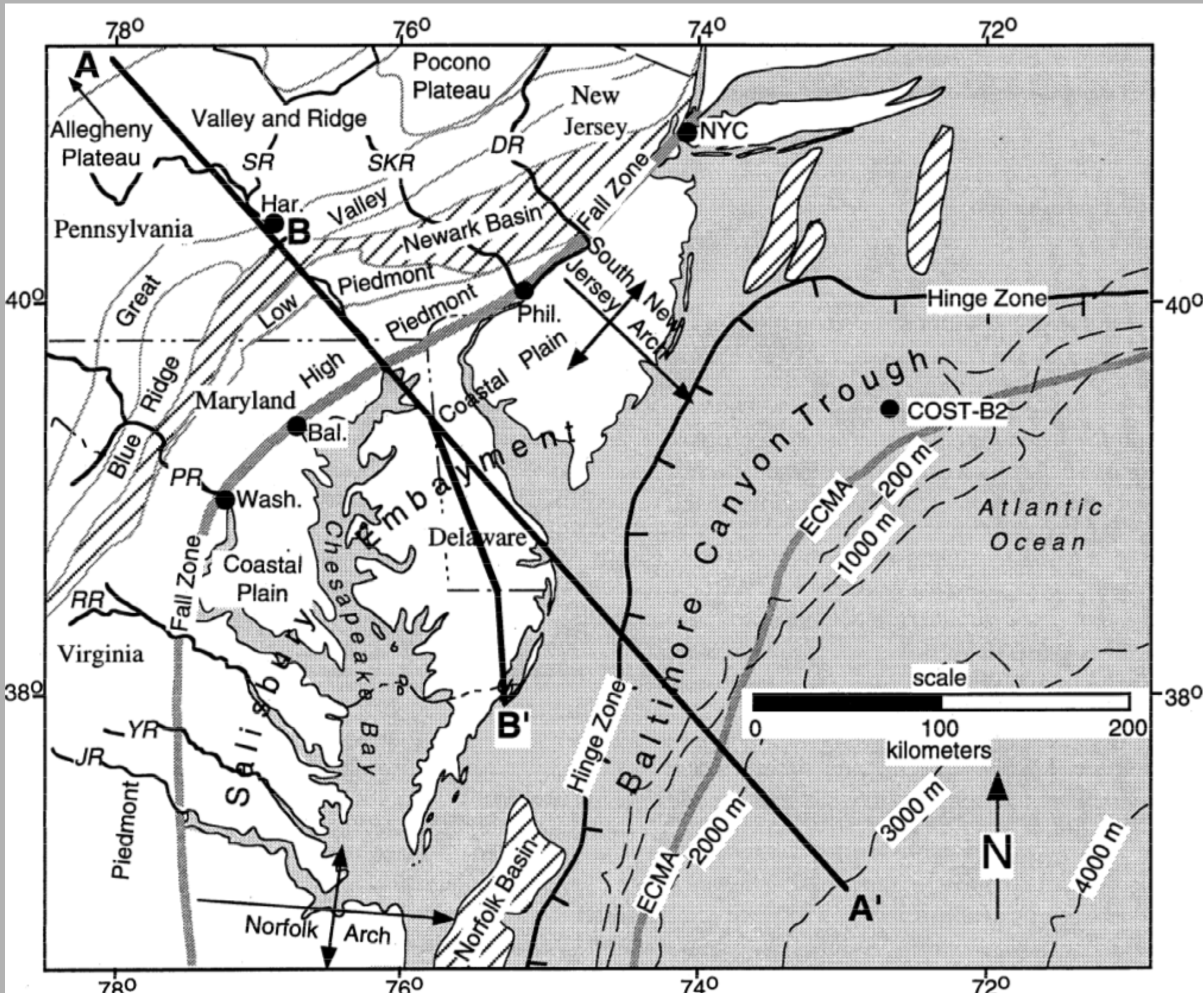

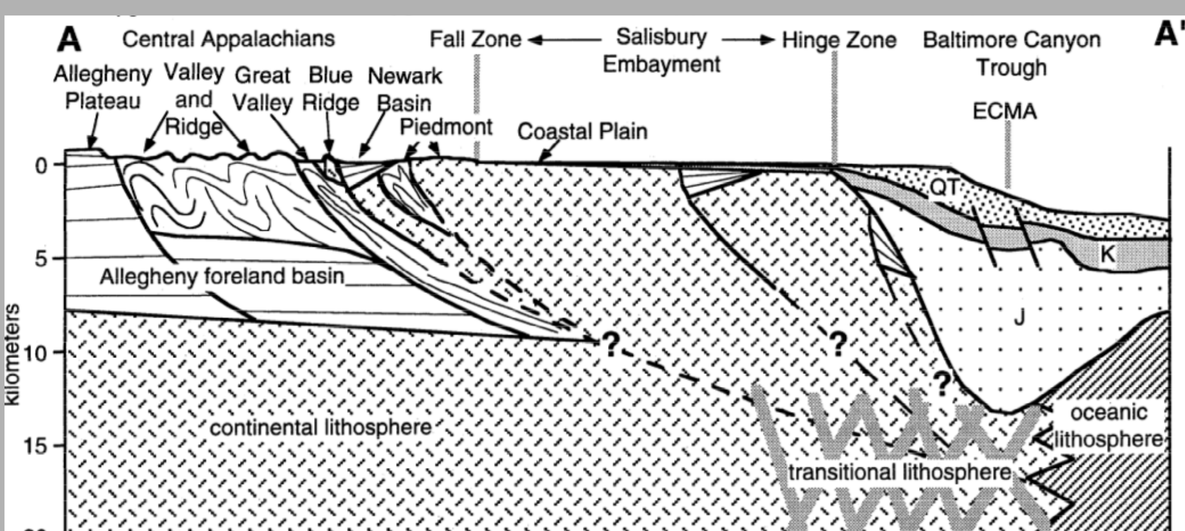

ENAM flexural deformation

Define:

- Fall Zone – transition from crystalline to sedimentary deposits
- Physiographic provinces

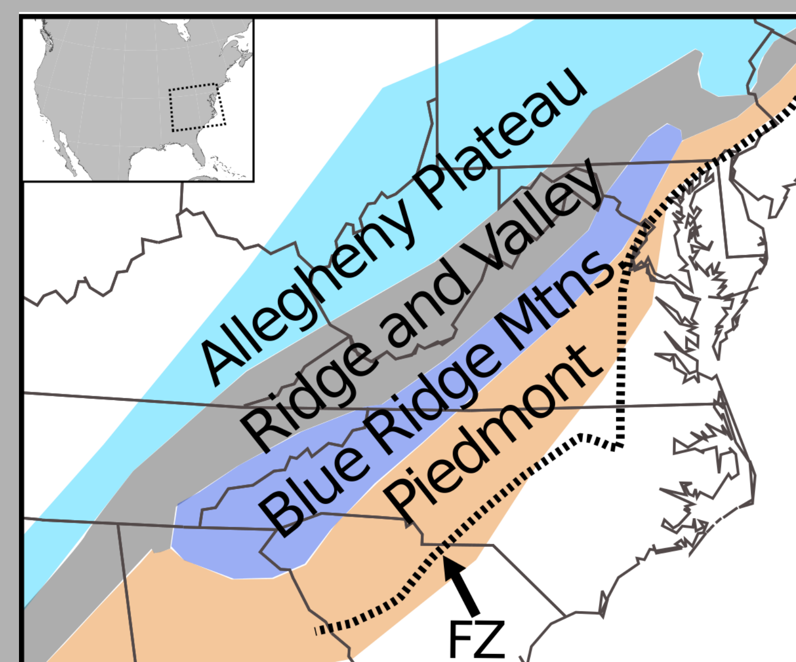

Pazzaglia and Gardner, 1994

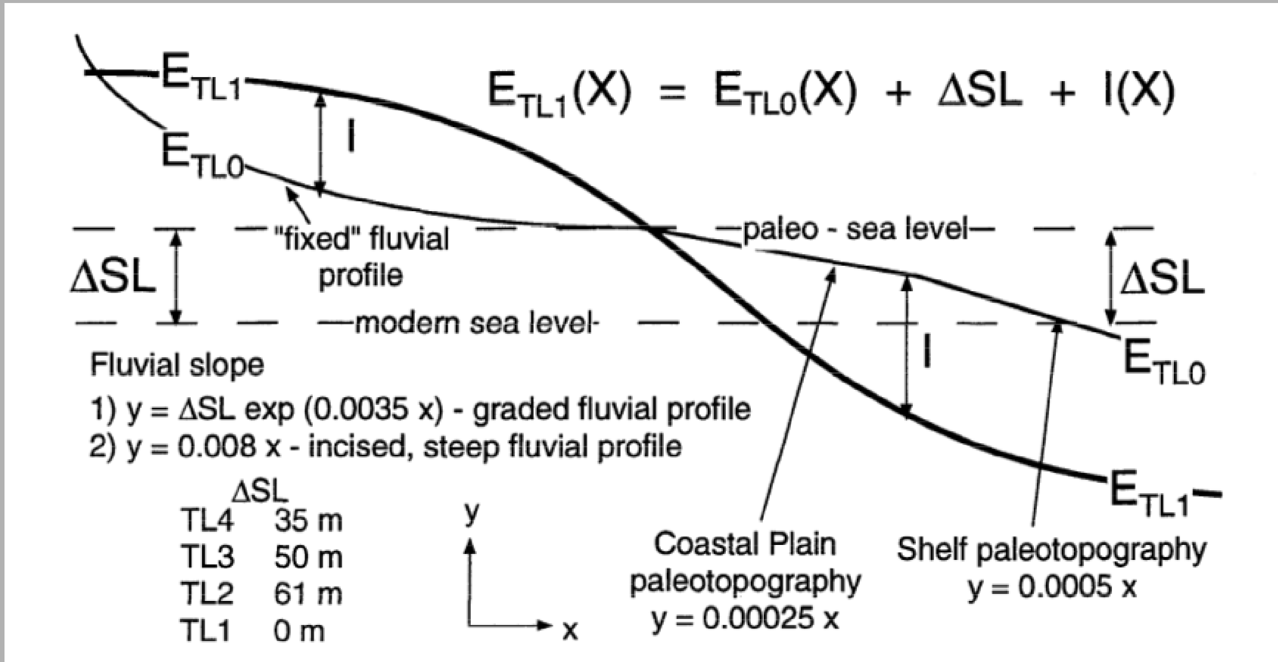

Figure 4. Graphical representation of the three basic components of model time lines.

- Time period: Late Cenozoic
  - Appalachians finished "building" ~180-200 Ma
- Time lines constrain model throughout deformation
- Variables: erosion rate and flexural rigidity

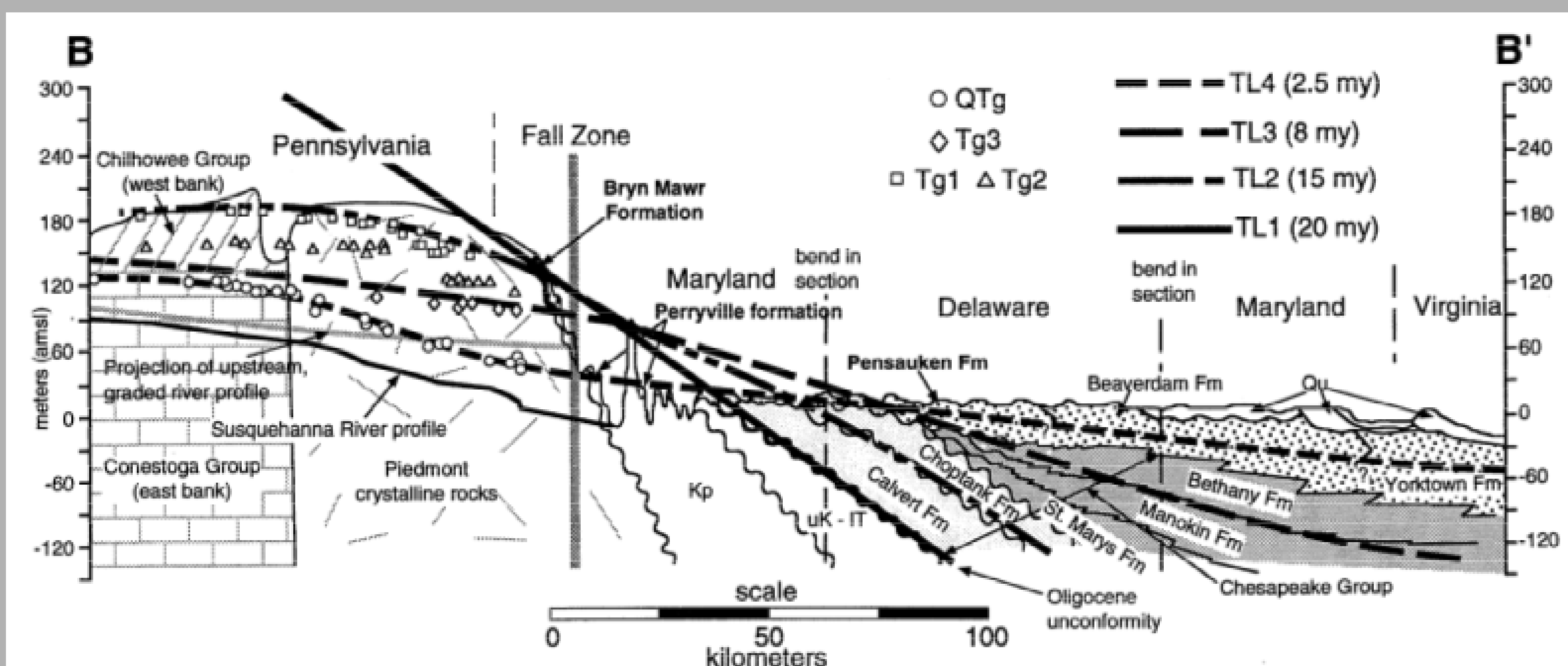

Results and implications

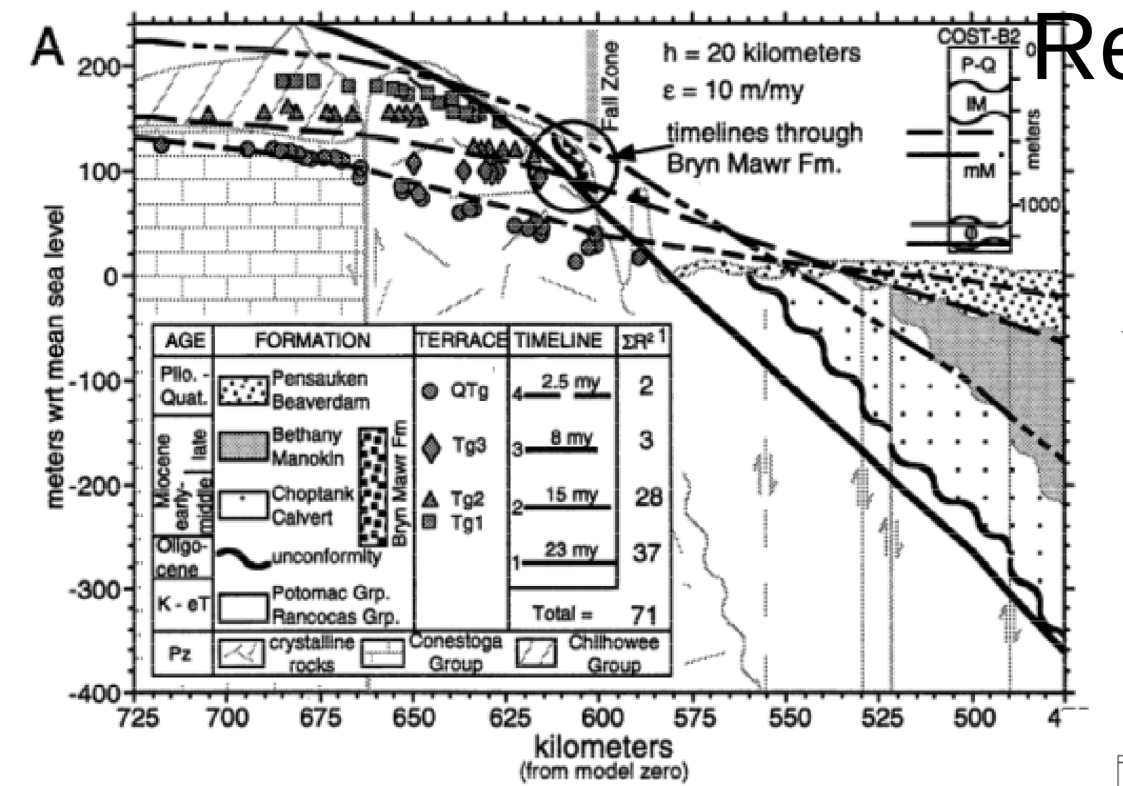

- Different stratigraphy generated by model, must match up
- Time line intersection is always near Fall Zone
  - i.e. the Fall Zone has been fixed through Late Cenozoic
- Lithology has likely had large impact on the extent/thickness of depositional facies
  - Penn. reentrant

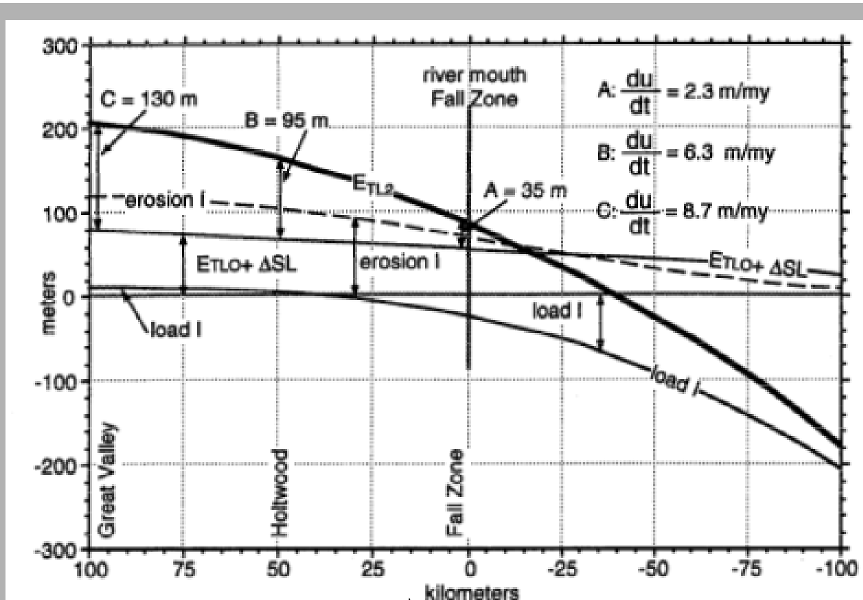

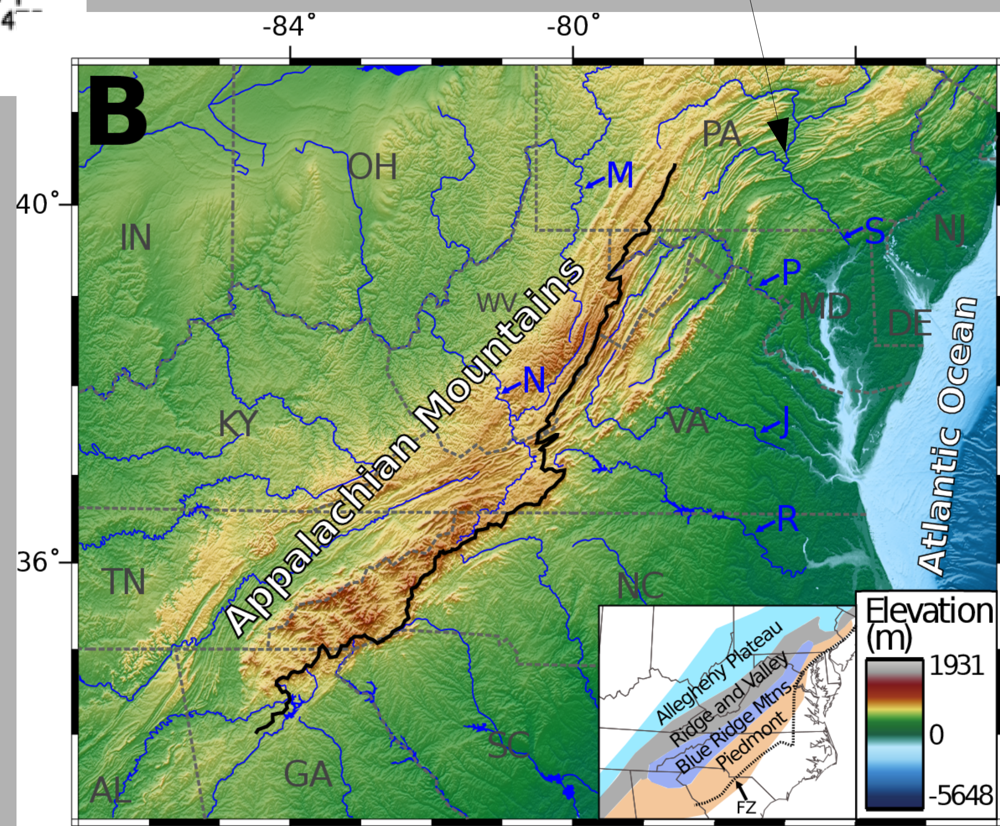

Uplift rate and magnitude increases away from bulge

Pazzaglia and Gardner, 2000

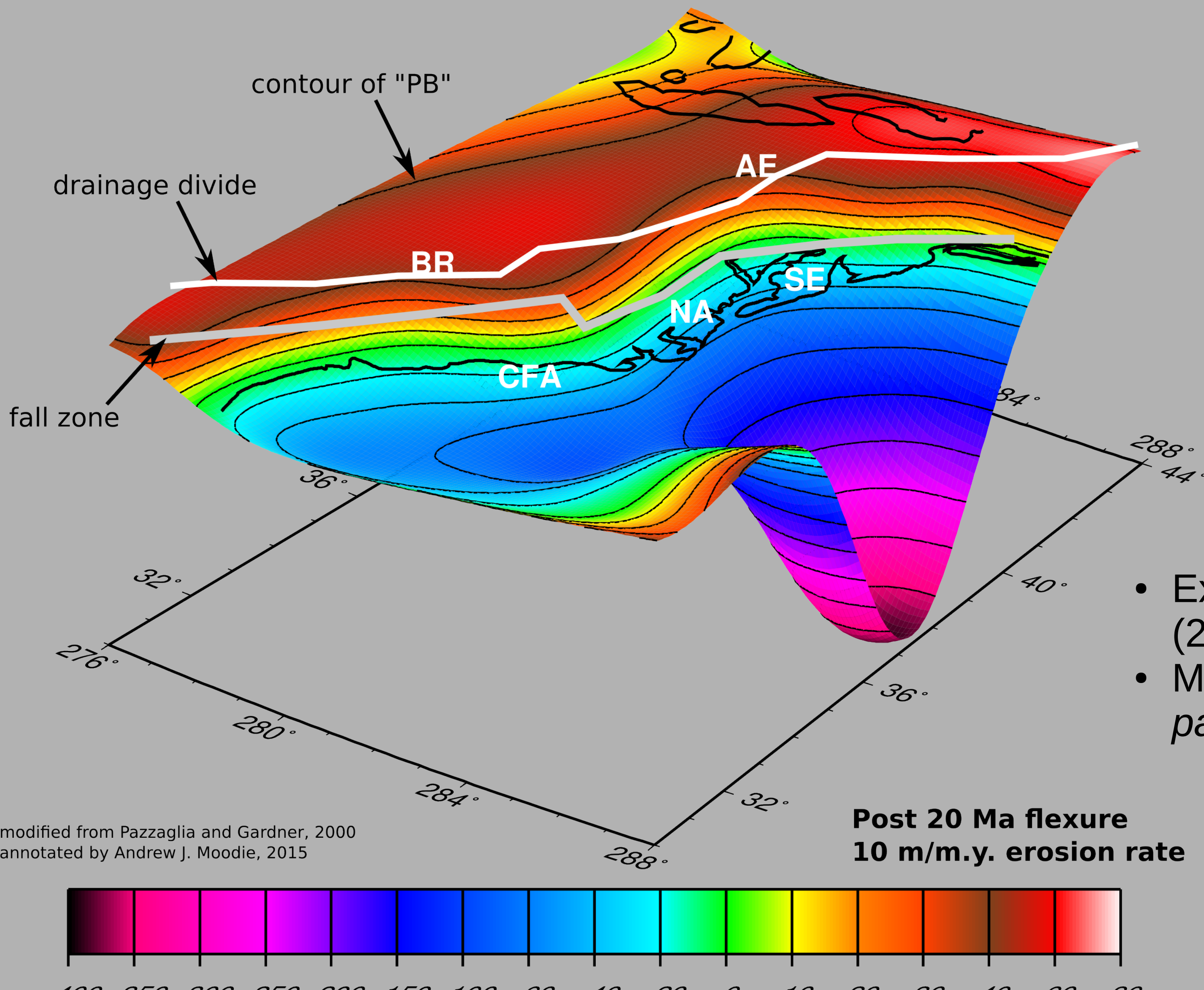

modified from Pazzaglia and Gardner, 2000
annotated by Andrew J. Moodie, 2015

- Extension of previous model (2D)
- Magnitude of deformation in a *passive* margin

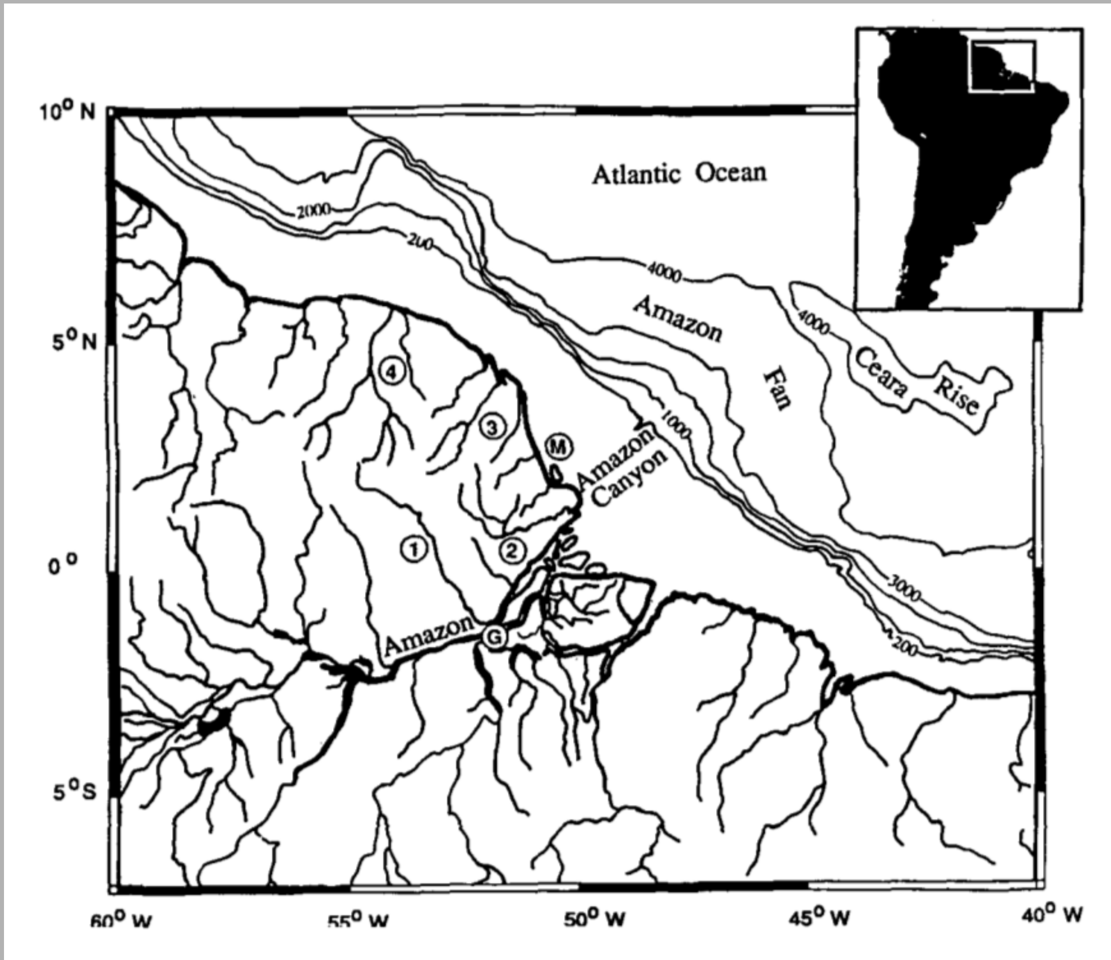

Driscoll and Karner, 1994

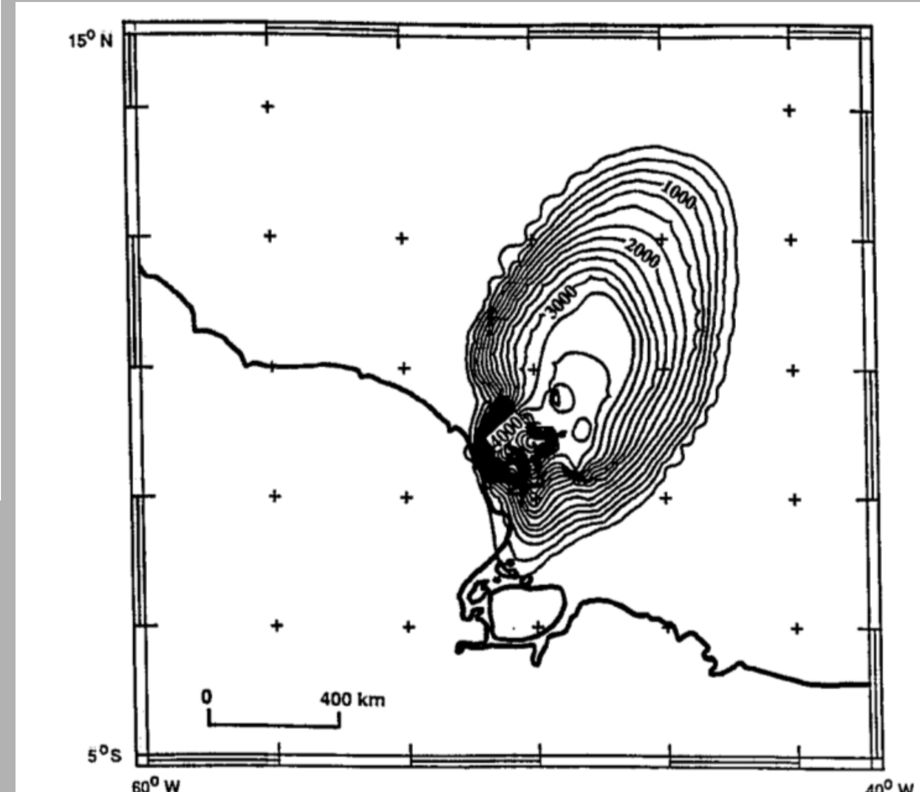

Figure 2. Isopach map of Amazon Fan for middle Miocene to present time. Contour interval is 250 m. Note that sediment thickness is markedly asymmetric and reaches maximum of 5300 m landward of present-day shelf edge. Crosses designate arbitrary modeling grid; projection scale is similar to Figure 1, and coastline is shown for ease of comparison.

Asymetric distribution of sediment in fan

Stratigraphic architecture?

Driscoll and Karner, 1994

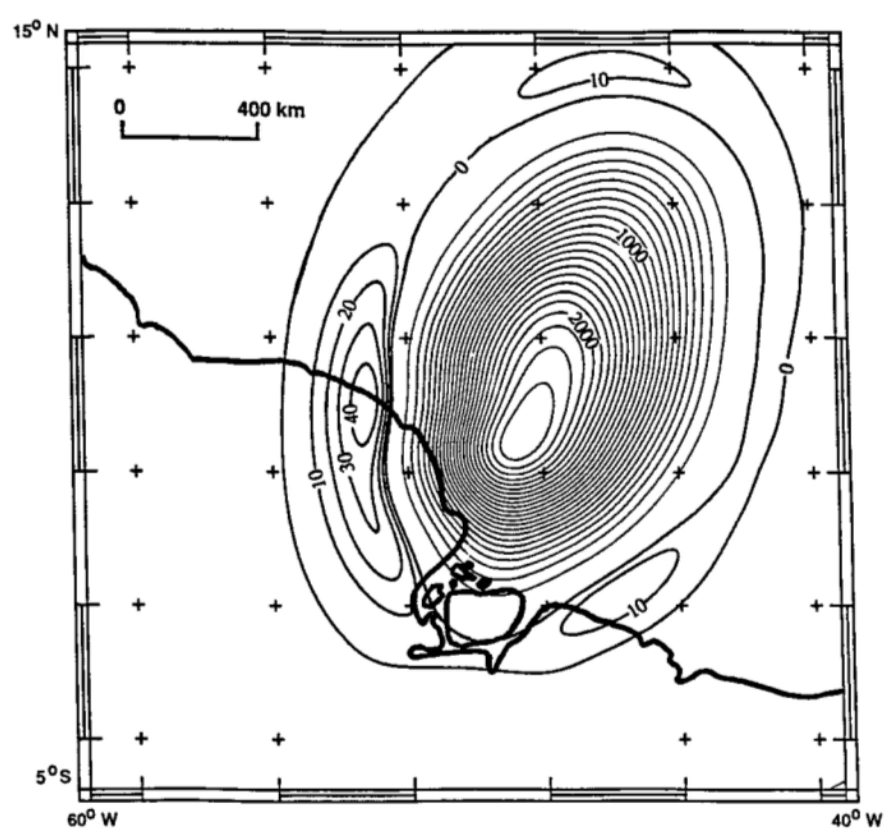

Figure 3. Calculated deflection for middle Miocene to present sediment loading shown in Figure 2. Contour interval for deflection is 100 m; for peripheral bulge it is 10 m. Peripheral bulge is asymmetric because load is asymmetric.

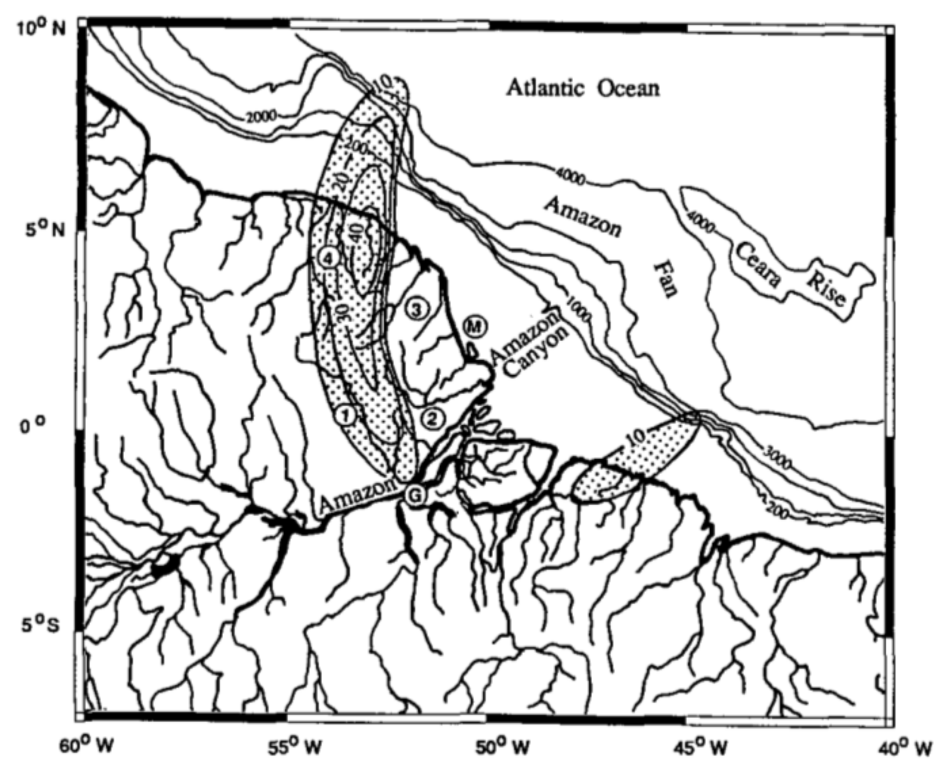

Figure 4. Calculated peripheral bulge is projected onto location map to examine spatial relation between flexural deformation and coastal drainage networks. Note that sources of headwaters of coastal rivers north of Amazon River are near crest of peripheral bulge.

- Stratigraphic implications
- Forcing of channel position
  - Channel stacking
  - Depocenter migration

Rouby et al., 2013

- Testing a numerical model for the evolution of passive margins – quasi 3D.
- Basically a large sensitivity analysis

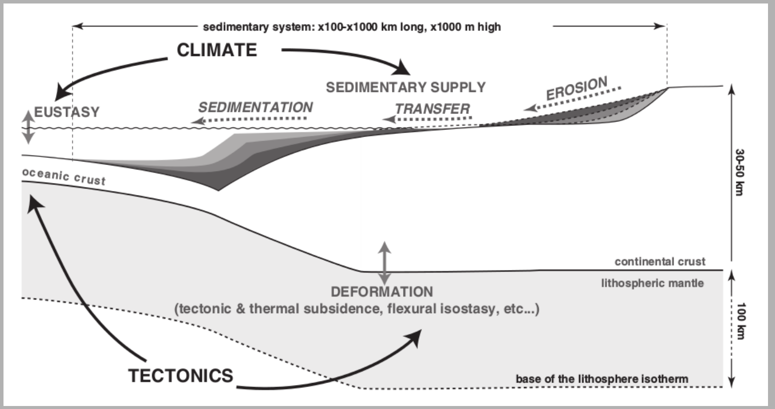

Parameter values and symbols used for the numerical experiments.

		Parameter tested	Kdc ($m^2\ Myr^{-1}$)	Kdw ($m^2\ Myr^{-1}$)	w_m (km)	z_n (km)	h^0_m (km)	T_L (°C)	δ/β	h^0_c (km)	T_l (°C)	ρ_s ($kg\ m^{-3}$)	ρ_m ($kg\ m^{-3}$)
Exp 0	Surface processes	*No surface processes*	0	0	250	25	100	1330	1	40	450	2400	3300
Exp 1		*Calibration of surface processes*	$3\ 10^{10}$	$3\ 10^{10}$	–	–	–	–	–	–	–	–	–
Exp 2			–	$3\ 10^{9}$	–	–	–	–	–	–	–	–	–
Exp 3		*Reference experiment*	$3\ 10^{10}$	$3\ 10^{8}$	250	25	100	1330	1	40	450	2400	3300
Exp 4			–	$3\ 10^{7}$	–	–	–	–	–	–	–	–	–
Exp 9		*Surface processes efficiency*	$3\ 10^{11}$	$3\ 10^{9}$	–	–	–	–	–	–	–	–	–
Exp 10			$3\ 10^{9}$	$3\ 10^{7}$	–	–	–	–	–	–	–	–	–
Exp 5	Lithosphere stretching	*Margin width*	$3\ 10^{10}$	$3\ 10^{8}$	150	–	–	–	–	–	–	–	–
Exp 6			–	–	600	–	–	–	–	–	–	–	–
Exp 7		*Depth of necking*	–	–	250	10	–	–	–	–	–	–	–
Exp 8			–	–	-	40	–	–	–	–	–	–	–
Exp 16		*Mantle/crust stretching ratio*	–	–	–	25	–	–	0.1	–	–	–	–
Exp 17			–	–	–	–	–	–	0.5	–	–	–	–
Exp 18			–	–	–	–	–	–	2	–	–	–	–
Exp 19			–	–	–	–	–	–	10	–	–	–	–
Exp 20			–	–	–	–	–	–	50	–	–	–	–
Exp 11	Lithosphere thermal state	*Lithosphere thickness*	–	–		–	150	–	1	–	–	–	–
Exp 12			–	–	–	–	200	–	–	–	–	–	–
Exp 14		*Lithosphere base temperature*	–	–	–	–	100	1300	–	–	–	–	–
Exp 15			–	–	–	–	–	1400	–	–	–	–	–
Exp 24		EET isotherm	–	–	–	–	–	1330	–	–	0	–	–
Exp 25			–	–	–	–	–	–	–	–	100	–	–
Exp 26			–	–	–	–	–	–	–	–	700	–	–
Exp 21	Lithosphere geometry	*Crust thickness*	–	–	–	–	–	–	–	36	450	–	–
Exp 22			–	–	–	–	–	–	–	38	–	–	–
Exp 23			–	–	–	–	–	–	–	42	–	–	–
Exp 27		Sediment density	–	–	–	–	–	–	–	40	–	2100	–
Exp 28			–	–	–	–	–	–	–	–	–	2700	–
Exp 29		Mantle density	–	–	–	–	–	–	–	–	–	2400	3400

Reference model

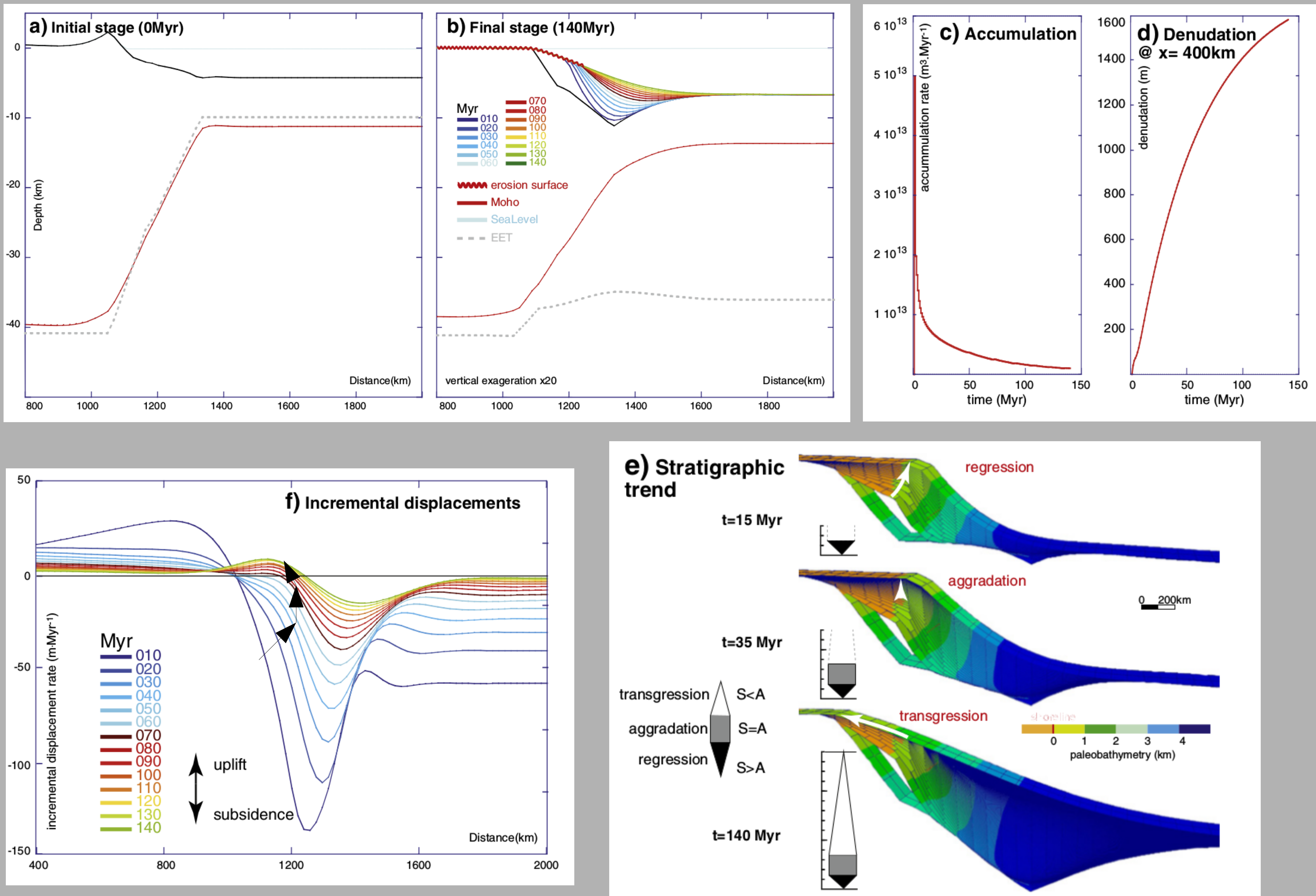

Surface process efficiency

Parameter values and symbols used for the numerical experiments.

		Parameter tested	Kdc ($m^2\ Myr^{-1}$)	Kdw ($m^2\ Myr^{-1}$)	w_m (km)	z_n (km)	h^0_m (km)	T_L (°C)	δ/β	h^0_c (km)	T_l (°C)	ρ_s (kg m^{-3})	ρ_m (kg m^{-3})
Exp 0	Surface processes	*No surface processes*	0	0	250	25	100	1330	1	40	450	2400	3300
Exp 1		*Calibration of surface processes*	$3\ 10^{10}$	$3\ 10^{10}$	–	–	–	–	–	–	–	–	–
Exp 2			–	$3\ 10^{9}$	–	–	–	–	–	–	–	–	–
Exp 3		*Reference experiment*	$3\ 10^{10}$	$3\ 10^{8}$	250	25	100	1330	1	40	450	2400	3300
Exp 4			–	$3\ 10^{7}$	–	–	–	–	–	–	–	–	–
Exp 9		*Surface processes efficiency*	$3\ 10^{11}$	$3\ 10^{9}$	–	–	–	–	–	–	–	–	–
Exp 10			$3\ 10^{9}$	$3\ 10^{7}$	–	–	–	–	–	–	–	–	–
Exp 5	Lithosphere stretching	*Margin width*	$3\ 10^{10}$	$3\ 10^{8}$	150	–	–	–	–	–	–	–	–
Exp 6			–	–	600	–	–	–	–	–	–	–	–
Exp 7		*Depth of necking*	–	–	250	10	–	–	–	–	–	–	–
Exp 8			–	–	-	40	–	–	–	–	–	–	–
Exp 16		*Mantle/crust stretching ratio*	–	–	–	25	–	–	0.1	–	–	–	–
Exp 17			–	–	–	–	–	–	0.5	–	–	–	–
Exp 18			–	–	–	–	–	–	2	–	–	–	–
Exp 19			–	–	–	–	–	–	10	–	–	–	–
Exp 20			–	–	–	–	–	–	50	–	–	–	–
Exp 11	Lithosphere thermal state	*Lithosphere thickness*	–	–		–	150	–	1	–	–	–	–
Exp 12			–	–	–	–	200	–	–	–	–	–	–
Exp 14		*Lithosphere base temperature*	–	–	–	–	100	1300	–	–	–	–	–
Exp 15			–	–	–	–	–	1400	–	–	–	–	–
Exp 24		EET isotherm	–	–	–	–	–	1330	–	–	0	–	–
Exp 25			–	–	–	–	–	–	–	–	100	–	–
Exp 26			–	–	–	–	–	–	–	–	700	–	–
Exp 21	Lithosphere geometry	*Crust thickness*	–	–	–	–	–	–	–	36	450	–	–
Exp 22			–	–	–	–	–	–	–	38	–	–	–
Exp 23			–	–	–	–	–	–	–	42	–	–	–
Exp 27		Sediment density	–	–	–	–	–	–	–	40	–	2100	–
Exp 28			–	–	–	–	–	–	–	–	–	2700	–
Exp 29		Mantle density	–	–	–	–	–	–	–	–	–	2400	3400

Calibrate erosion rate (diffusion) with records, and then test to confirm validity.

accumulation rate

$$V = V_o . e^{-\frac{1}{\tau}t}$$

relaxation time

Wavelength of relief being eroded

$$K_d = \frac{L^2}{\tau}$$

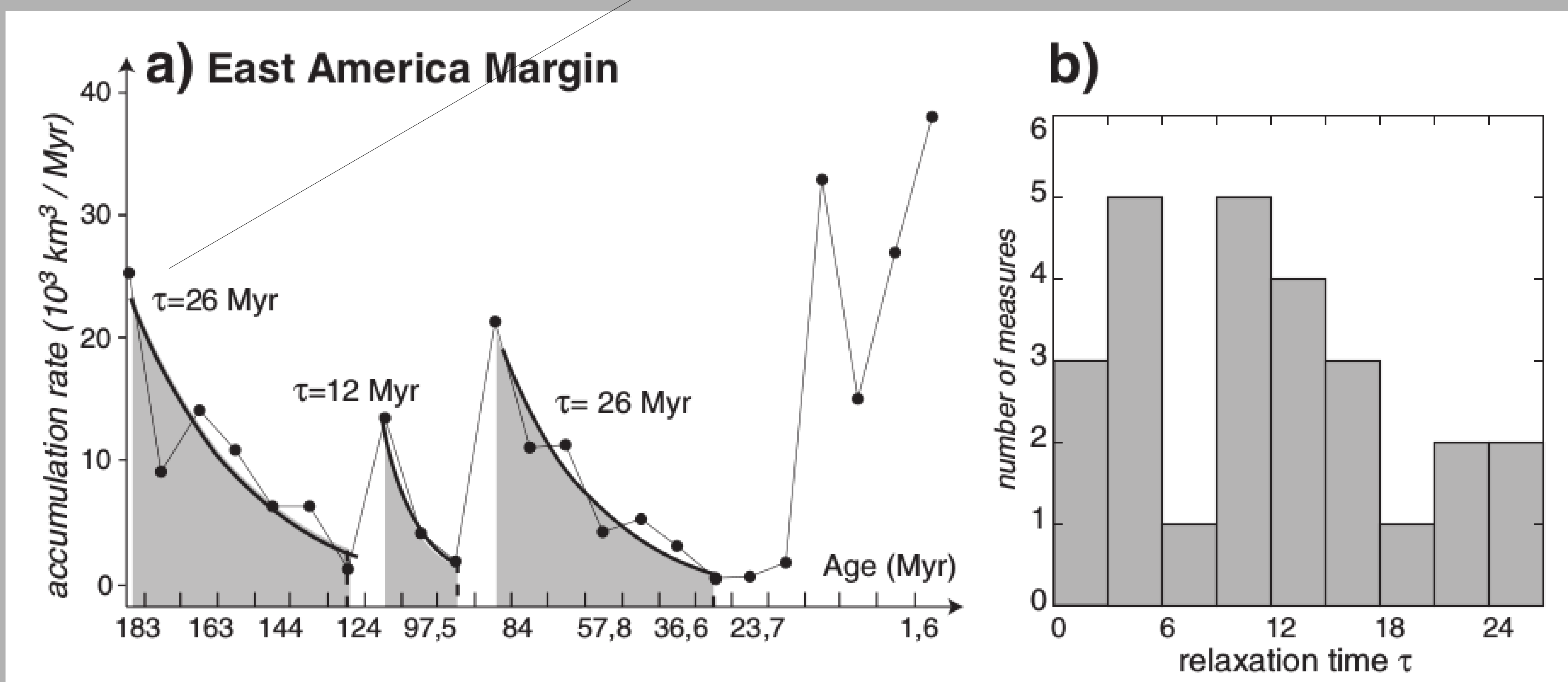

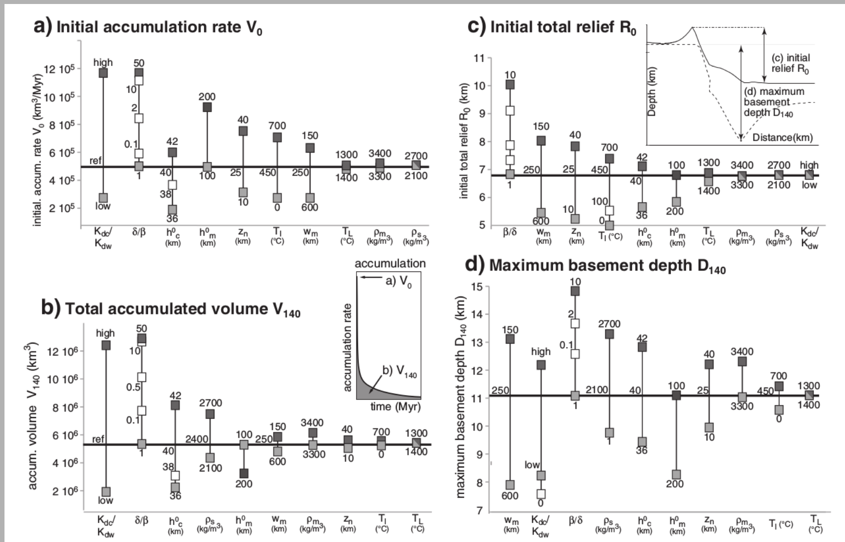

measurement
metrics

and stratigraphic phases!

Surface process efficiency

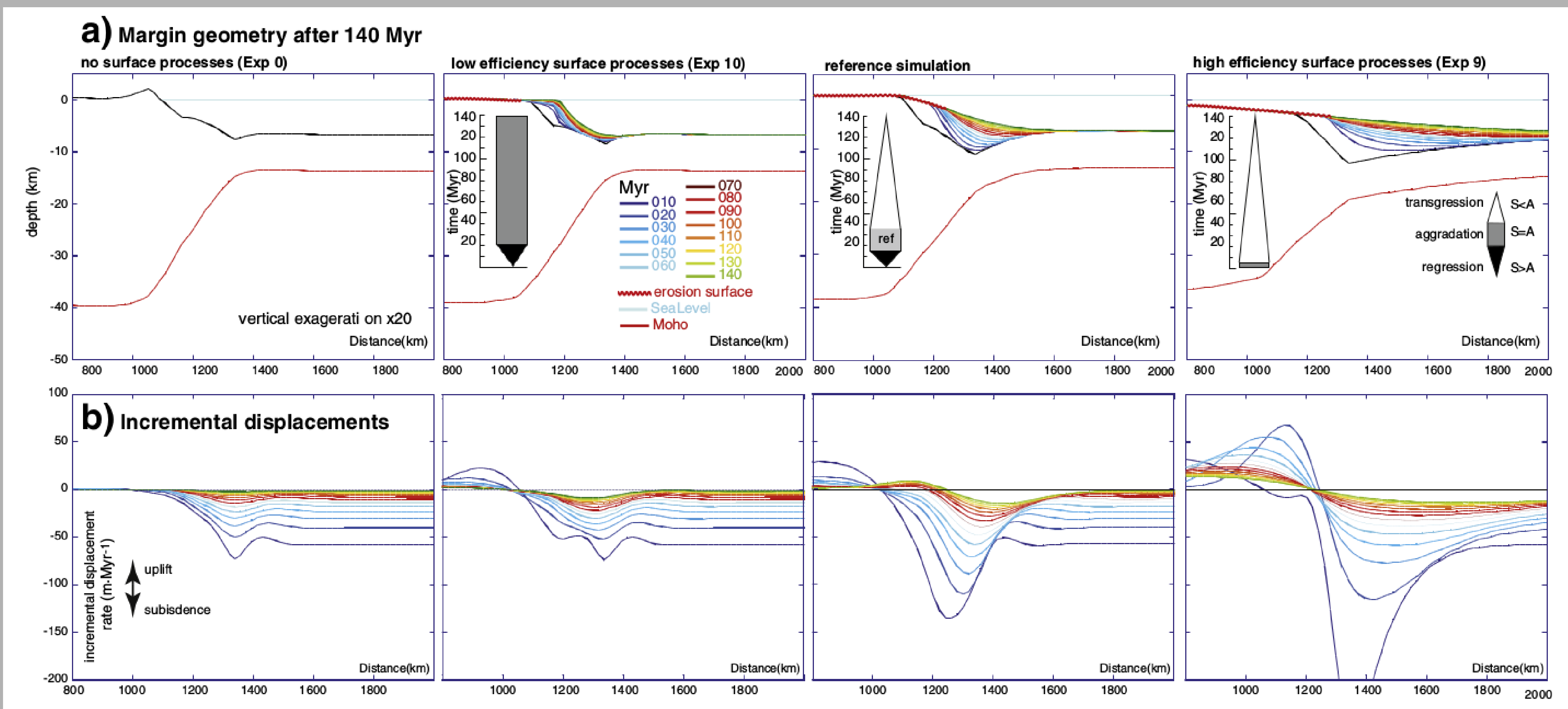

Big impact results

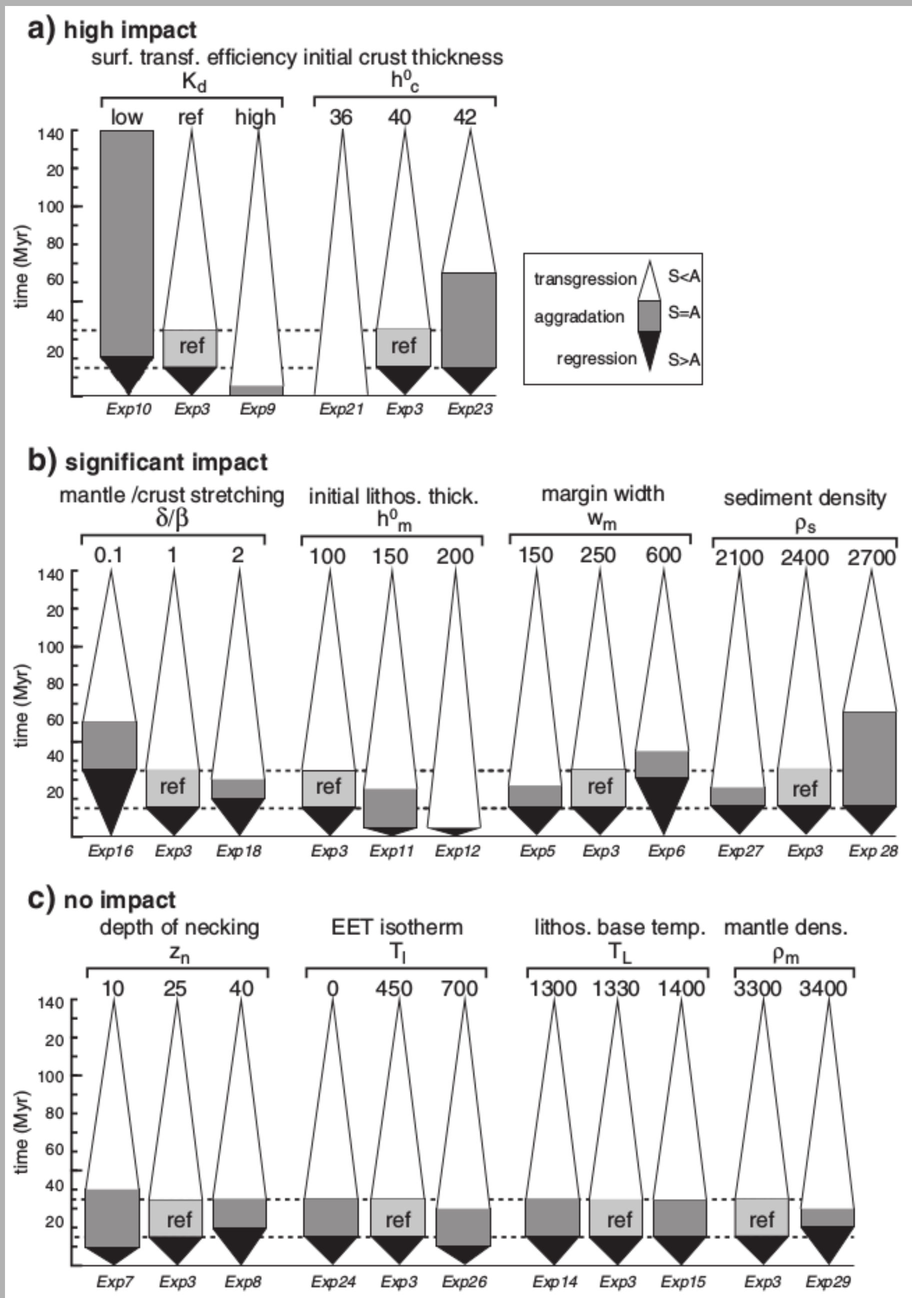

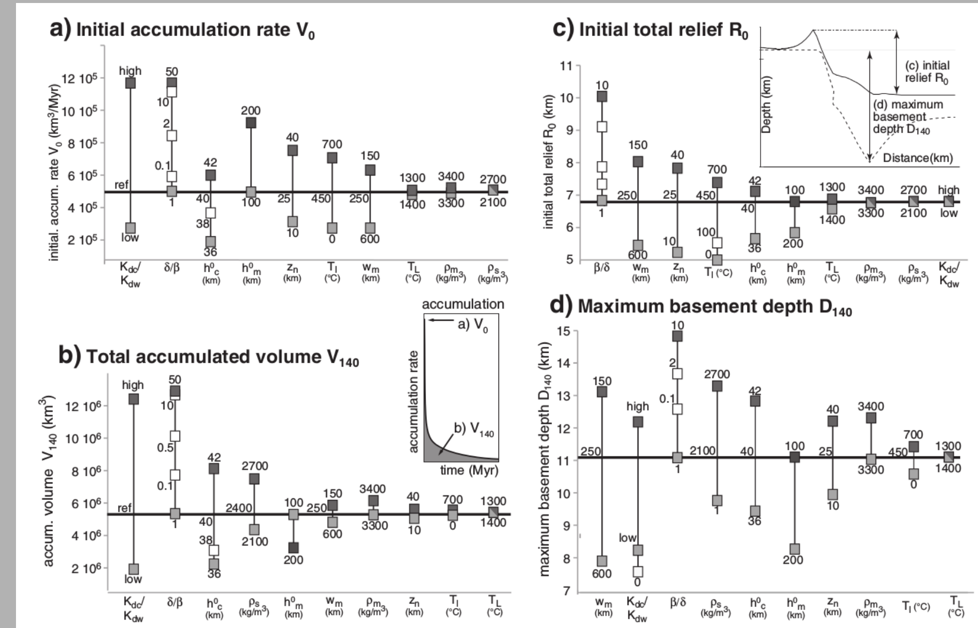

- Almost all dominated by transgression
- Impactors, in order:
  - Efficiency of surf. processes
  - Initial crust thickness
  - Sediment density
  - Following most affects initial stages
    - Depth-variable stretching
    - Margin width
    - Lithosphere thickness
    - Depth of necking
    - EET isotherm
    - Lithosphere basal temp, mantle density

gressive trends during the post-rift of Atlantic-type basins. Thus, the view of long-term stratigraphic trend of passive margins mostly driven by an exponentially decreasing rate of the thermal subsidence and a sedimentary supply larger than the space available for sedimentation ("over-filled" margins) should be revised to include the impact of the flexural component of the isostatic response of the stretched lithosphere on both the accommodation and the accumulation histories. A passive margin showing a flexural response is expected to display both accumulation and accommodation rates decreasing exponentially through time. More regional boundary conditions affecting surface processes (e.g. drainage, precipitation) and lithosphere flexure (e.g. lithosphere and crust thicknesses, margin width and depth dependency of stretching) control the relative decreasing rates of accommodation, that is to say, the long-term stratigraphic trend of the sedimentary wedge. Alternatively, the long-term regressive trends observed during the post-rift of many Atlantic-type basins suggest that those margins must have undergone other events, altering either the long-term accumulation histories (major drainage area reorganization durably increasing the terrigeneous input or major increase in the in-situ sediment production) or the long-term subsidence (dynamic topography or thermal anomalies limiting the accommodation creation).

Crust

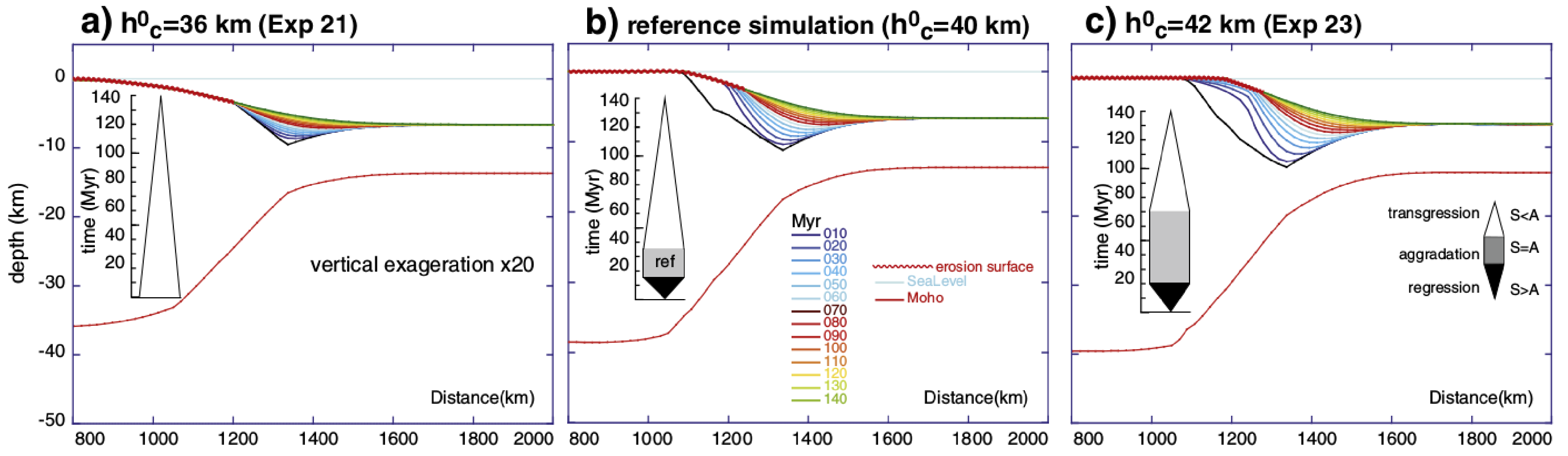

Margin width

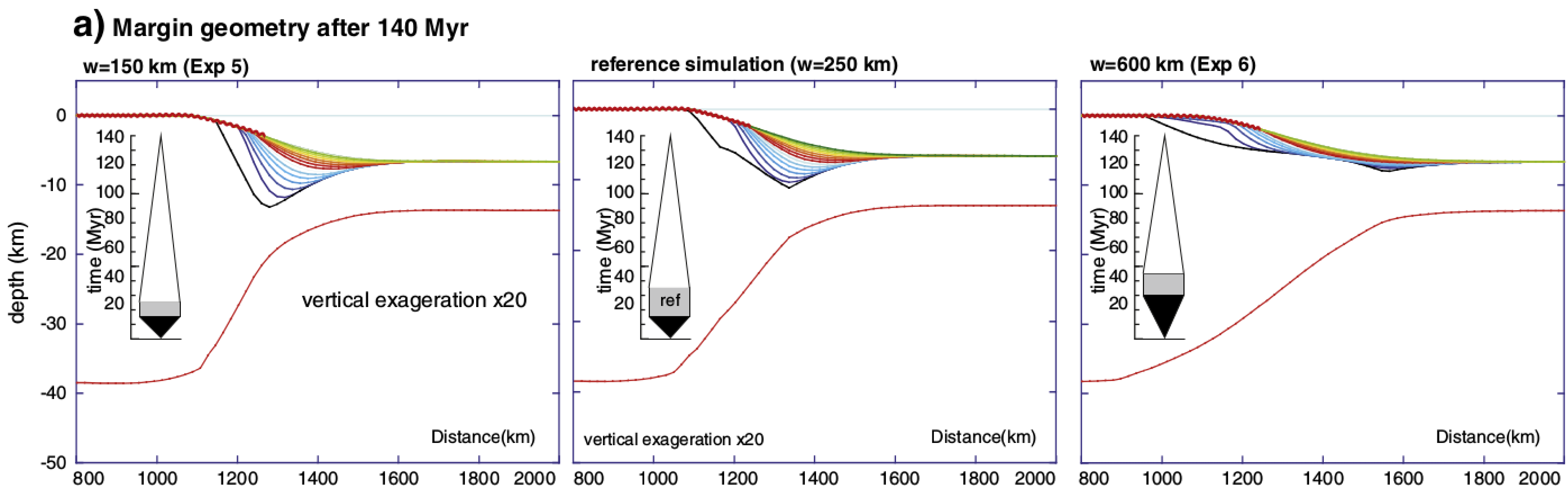

Isostatic deformation will be calculated by a geodynamic model that simulates the lithosphere as an infinite, unbroken, elastic plate of uniform thickness. The approximation of flexure for a thin, unbroken elastic plate [*Turcott and Schubert*, 1982] is:

$$\frac{Dd^4W}{dx^4}+\frac{Pd^2W}{dx^2}+(\rho_m-\rho_s)gW=q \tag{2}$$

where D is flexural rigidity, P is horizontal stresses, W is vertical stresses, ρ_m is lithosphere density, and ρ_s is sediment density. Assuming the absence of horizontal stresses ($P = 0$) and a uniform-thickness plate (D = constant), this differential equation has a well-known one-dimensional analytic solution:

$$\boxed{W_b(x)=W_o e^{-x/\alpha}\left(\cos\frac{x}{\alpha}+\sin\frac{x}{\alpha}\right)} \tag{3}$$

where W_o is the deflection at the point of loading or unloading, x is the distance along the plate, $W_b(x)$ is deflection of the plate at point x from W_o, and α is the flexural parameter defined by plate flexural rigidity. The flexural parameter and flexural rigidity are related by:

$$D=\frac{Eh^3}{12\left(1-\upsilon^2\right)} \tag{4}$$

$$\alpha^4=\frac{4D}{\rho_m g} \tag{5}$$

where E is the plate elasticity (parameterized as 70 X 10^9 Pa), v is Poisson's ratio (parameterized as 0.25), and h is the elastic thickness.

Plate deflection at the point of loading (or unloading) (W_o) is defined as

$$W_0=\frac{q\alpha^3}{8D} \tag{6}$$

where

$$q = \rho_s\, g\, \Delta x\, y \qquad (7),$$

g is acceleration of gravity (9.81 m/s^2), and $\Delta x\ y$ is the cross-sectional area of the load.